

SEMICONDUCTORS  
AND DIELECTRICS

## Investigation of the Structure, Physical Properties, and Phase Transition in SrAlF<sub>5</sub>

S. V. Mel'nikova<sup>a,\*</sup>, L. I. Isaenko<sup>b,\*\*</sup>, M. V. Gorev<sup>a</sup>, A. D. Vasil'ev<sup>a</sup>, and S. I. Lobanov<sup>b</sup>

<sup>a</sup> Kirensky Institute of Physics, Siberian Branch, Russian Academy of Sciences, Akademgorodok, Krasnoyarsk, 660036 Russia

\* e-mail: msv@iph.krasn.ru

<sup>b</sup> Trofimuk United Institute of Geology, Geophysics, and Mineralogy, Siberian Branch, Russian Academy of Sciences,  
pr. Koptyuga 3, Novosibirsk, 630090 Russia

\*\* e-mail: lisa@uigmm.ncs.ru

Received April 16, 2009; in final form, August 1, 2009

**Abstract**—Crystals of SrAlF<sub>5</sub> have been grown by the Bridgman method from the melt and by sintering of the components. Optical polarization studies and measurements of the thermal expansion and birefringence coefficients have been carried out over a wide temperature range. The electromechanical coefficient  $d_{33}$  has been measured, and the optical second harmonic, dielectric hysteresis loop, and optical quality of the crystal have been assessed. X-ray diffraction investigations have been performed to identify the revealed compounds. It has been demonstrated that the SrAlF<sub>5</sub> crystals obtained under the growth conditions chosen have  $I4_1/a$  symmetry and do not undergo structural phase transitions in the temperature range 100–800 K. Crystalline inclusions of the AIOF oxyfluoride have been revealed in crystals grown with an AlF<sub>3</sub> excess. The birefringence of the AIOF crystal is an order of magnitude higher than that of SrAlF<sub>5</sub>, does not depend on temperature, and has no anomalies up to 800 K.

DOI: 10.1134/S1063783410030108

### 1. INTRODUCTION

Fluorine compounds have become recently subjects of intense research as possible candidates for a variety of optical applications due to their inherent unique properties, such as transparency over a wide spectral range, high resistance to optical damage, and a possibility of doping by trivalent rare-earth ions. Studies of the phase diagram of the SrF<sub>2</sub>–AlF<sub>3</sub> system [1–3] revealed a series of compounds: monoclinic  $\alpha$ -SrAlF<sub>5</sub> [1], tetragonal  $\beta$ -SrAlF<sub>5</sub> [2], tetragonal Sr<sub>2</sub>AlF<sub>7</sub>, and orthorhombic Sr<sub>3</sub>Al<sub>2</sub>F<sub>16</sub> [3].

Tetragonal  $\beta$ -SrAlF<sub>5</sub> (SAF) has a transparency window of 0.16–10  $\mu\text{m}$  [4] and is tentatively considered for use as a matrix crystal for tunable solid-state lasers for operation in the UV, visible, and IR regions of the spectrum [5–7]. It is also viewed as a candidate material for use in the quasi-phase matching technique in frequency conversion problems [4, 8]. The latter idea draws from studies [9, 10] which, based on the structural data and  $I4$  (or  $P4$ ) symmetry group of the crystal, suggested possible realization of the ferroelectric phase in this crystal, predicted a ferro- to paraelectric phase transition at  $T_0 \approx 685$  K, and calculated the spontaneous polarization  $P_s \approx 9$ –48  $\mu\text{C}/\text{cm}^2$ . One has also forwarded persuasive experimental evidence for the existence of a persistent ferroelectric state at room temperature; more specifically, one measured the electromechanical coefficient  $d_{33} \approx$

$0.1$ – $0.8 \times 10^{-12}$  C/N (the scatter in the values of  $d_{33}$  for different samples should be assigned to the influence of domains), detected optical second harmonic generation (SHG) at the intensity level characteristic of quartz on powder samples [10], and observed a dielectric hysteresis loop [4]. Anomalies were also observed in the heat capacity, dielectric permittivity [10], and birefringence [11] near 700 K.

At the same time, there is a host of publications, including structural measurements, which demonstrate inversion symmetry in this crystal, thus making the existence of the ferroelectric state impossible [12–14]. Two possible centrosymmetric versions of SAF crystal symmetry at room temperature were considered:  $I4/m$  with the parameters  $a = b = 14.059$  Å,  $c = 7.1612$  Å,  $Z = 16$  (small cell) and  $I4_1/a$  with  $a = b = 19.882$  Å,  $c = 14.322$  Å,  $Z = 64$  (large cell) [12]. The first structural version assumes a disordered fluorine atomic arrangement in [Al<sub>2</sub>F<sub>10</sub>] dimer anion groups, whereas in the second version, the fluorine atoms are ordered. The  $I4_1/a$  symmetry group is believed [12] preferable because of observation of weak superstructure ( $hkl$ ) reflections, where  $l = 5$ . Investigation of polarized Raman and IR spectra also revealed the existence of inversion symmetry in the crystal [13]. Studies of the dielectric properties and electrical conductivity [14] provided supportive evidence for the existence of an anomaly in low-frequency permittivity at temperatures  $T_{0\uparrow} = 715$  K and  $T_{0\downarrow} = 710$  K in the

region of the hypothetical  $I4_1/a \leftrightarrow I4/m$  structural phase transition accompanied by ordering of fluorine atoms in the  $[Al_2F_{10}]$  complexes. It was shown that the conductivity of the crystal, both along the fourfold symmetry axis and perpendicular to it, increases by four orders of magnitude in the temperature range from room temperature to  $\sim 750$  K. This increase in the concentration of charge carriers with temperature provided grounds for identifying this compound with solid electrolytes [14].

Thus, despite a large number of studies, the available results appear to be at variance. This relates both to the presence or absence of inversion symmetry in the crystal and to interpretation of the reported observations. Indeed, the unusual shape of the dielectric hysteresis loop [4] which did not permit determination of the coercive field is believed [14] rather to suggest conduction in the sample. Powder samples revealed generation of the optical second harmonic [4, 8, 10], while measurements of the SHG level and the electrooptical coefficients on single crystals of good optical quality produced a negative result [14]. The crystals used in studies were melt grown by different techniques. The loss of  $AlF_3$  in the growth induced by its volatility was countered by different methods. When growing in a closed volume, the loss of  $AlF_3$  was counteracted by maintaining an enhanced gas pressure over the melt [11–15]. In the Czochralski method [4, 8, 15], the starting off-stoichiometry of the charge was as high as 40%. It was shown that the crystals produced in this way could include both oxide and oxyfluoride phases [15].

We report here on a study of the physical characteristics of the SAF crystal, more specifically, its thermal expansion and birefringence within a wide temperature range (400–800 K), in an attempt to gain insight into the nature of the phase transition in the vicinity of 700 K. The electromechanical coefficient has been measured, and the second harmonic and optical quality of the crystal investigated. The experiments were conducted on samples grown by different methods and at different stoichiometry levels. The X-ray structural measurements performed provided unambiguous identification of the compounds.

## 2. SAMPLE PREPARATION AND EXPERIMENTAL TECHNIQUE

The crystals for the study were grown from the melt of the starting components,  $AlF_3$  (99.99) and  $SrF_2$  (99.99), at high temperatures ( $\sim 1600$  K) or by their sintering at comparatively low ones. Because of the high volatility of  $AlF_3$  which could interfere with crystal growth by the Bridgman method, the sublimation was suppressed by maintaining an excess pressure in the vessels by filling them with  $N_2$ , as well as by adding  $CF_4$  (99.99) as a fluorine agent into the reactor. As a result, the pressure maintained in the vessel was in

excess of one atmosphere. All operations were performed in a dry environment to exclude contamination with oxygen-containing impurities. The growth was carried out in a glassy graphite container which was treated adequately and placed in a quartz vessel. The vessel was placed in a two-zone furnace, with the temperature gradient near the crystallization front of 10–20 K/cm at  $T \approx 1050$  K. In the course of growth from melt, experiments with different fractions of the starting components were conducted. In one of such experiments (no. 1), an  $AlF_3$  excess (about 2 wt. %) was added during crystallization to the starting reaction mixture. This was followed by multiple recrystallization of the material thus obtained, with sampling of the most transparent fraction (sample no. 2). Crystallization experiment no. 3 consisted in adding 5 wt. % of  $AlF_3$  to the material of crystallization no. 2. The fourth crystallization was effected with a stoichiometric charge. Crystallization lot no. 5 was obtained by sintering the starting components in a closed graphite crucible. Fast heating was performed up to a temperature of  $\approx 1170$  K, after which the furnace was switched off. The material thus obtained was actually a ceramic with a hollow filled by transparent needle-shaped crystals with a square cross section and 1–2 mm long.

The optical quality of the transparent single crystals prepared was studied with an Axioskop 40 Pol polarization microscope, with Plan-Neofluar (Zeiss) objectives providing high resolution and contrast. The samples were oriented platelets measuring  $1.5 \times 4.5 \times 4.5$  mm (no. 1) and  $2.25 \times 4.53 \times 5.00$  mm (no. 2), and (100)-cut platelets of crystallization materials nos. 3 and 4. We studied also a single crystal found in the material of crystallization lot no. 5 which was  $0.48 \times 0.42 \times 2.00$  mm in size. The main birefringence  $\Delta n = n_e - n_o$  was measured on samples nos. 1–5 with the use of a Berek compensator (Leica), with an accuracy of  $\pm 10^{-5}$ , and a Senarmont compensator, providing a sensitivity of  $\sim 10^{-7}$ , at the wavelength of the helium–neon laser ( $\lambda = 6328 \text{ \AA}$ ). The thermal expansion coefficients were measured on sample no. 2 along the three orthogonal directions with a DIL 402C dilatometer (NETZSCH) in dynamic mode in air, at a heating rate of 3–5 K/min. To calibrate the measuring system and take into account properly its thermal expansion, the measurements were referenced against fused quartz and corundum standards. The structural data were obtained with a SMART APEX II X-ray autodiffractometer with an  $x$ – $y$  CCD detector ( $MoK_\alpha$  radiation). The measurements were performed up to  $2\theta_{\max} = 58^\circ$ .

Studies in polarized light revealed considerable differences among the samples prepared. The crystals grown stoichiometric (nos. 2 and 4) exhibit even and distinct extinction, whereas in samples nos. 1 and 3 the extinction was uneven because of the block structure, systematic bands, and crystalline inclusions (Fig. 1a). Figure 1b demonstrates a region of the crystal with large inclusions specified by dashed lines. We readily

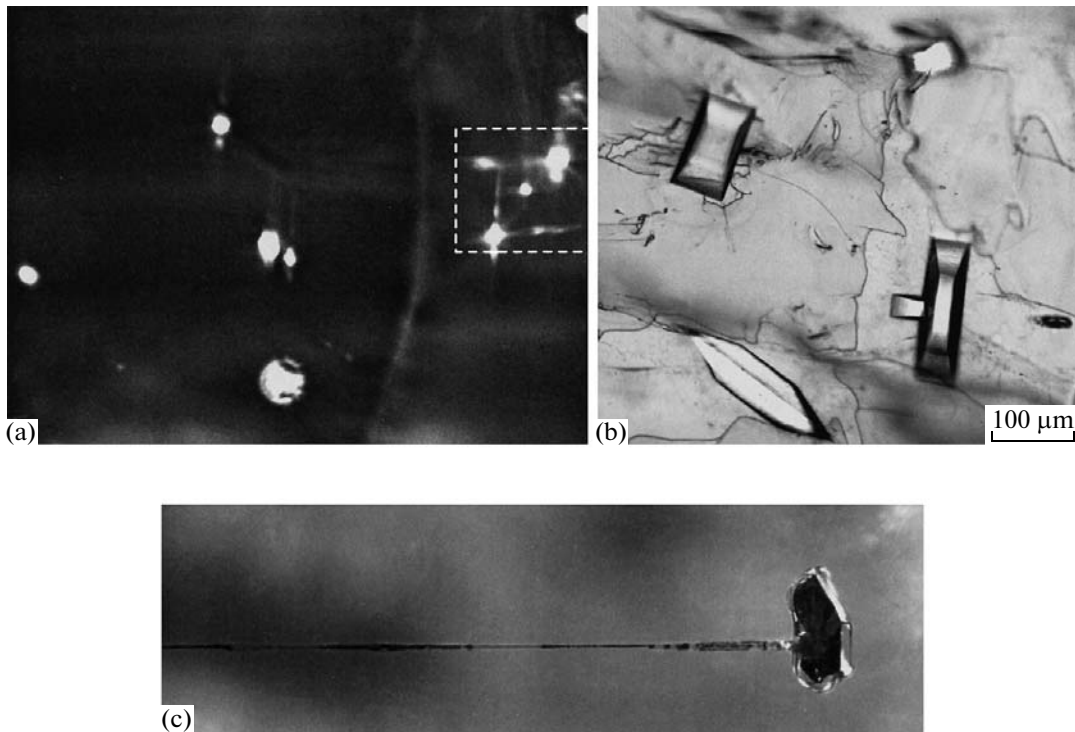


**Fig. 1.** Examination of  $\text{SrAlF}_5$  (100)-cut platelets in polarized light: (a) uneven extinction in samples nos. 1 and 3 due to the block structure, systematic bands, and crystalline inclusions; (b) region of the sample with large inclusions identified by dashed lines in panel (a); and (c) shape of defects of stoichiometrically grown samples (nos. 2, 4).

see that they represent actually faceted crystallites of different size, which are distributed nonuniformly over the volume of the matrix material. The interference color scale suggests that the path difference in the crystallites corresponds to a birefringence an order of magnitude larger than that of the matrix material. Whence it follows that growth with excess  $\text{AlF}_3$  favors the formation of crystals of unknown composition in the matrix of the main material. It was found that repeated heatings to 800 K bring about increasingly more intense cracking of the matrix material near its contact with the crystallites. A closer study revealed defects, fairly few in number, in samples nos. 2 and 4. They were identified, however, as capsules, empty or filled by a nontransparent material, resembling channels, parallel to [001] and exiting onto the surface (Fig. 1c).

Figure 2 plots the results of measurements of thermal expansion coefficients for sample no. 2. The coefficient  $\alpha_a$  varies in the course of heating from  $14 \times 10^{-6} \text{ K}^{-1}$  at 400 K to  $17.5 \times 10^{-6} \text{ K}^{-1}$  at 750 K (Fig. 2, curve 1), and  $\alpha_c$ —from  $10 \times 10^{-6}$  to  $15 \times 10^{-6} \text{ K}^{-1}$ , respectively (Fig. 2, curve 2). Repeated measurements conducted in the [100] direction show the reproducibility of the values and the measurement error. The measurements of  $\alpha_a$  performed along the short length exhibiting a large error (of the order of  $\pm 5\%$ ), they are not plotted here. No anomalies in the thermal expansion coefficients along [100] and [001] in excess of the

measurement error have been found within the temperature region covered.

In order to measure birefringence on samples nos. 1 and 3, regions with a small number of inclusions and exhibiting good extinction were chosen. One measured the birefringence of the matrix crystal, because that of the crystalline inclusions was excluded by the experimental conditions. At room temperature,

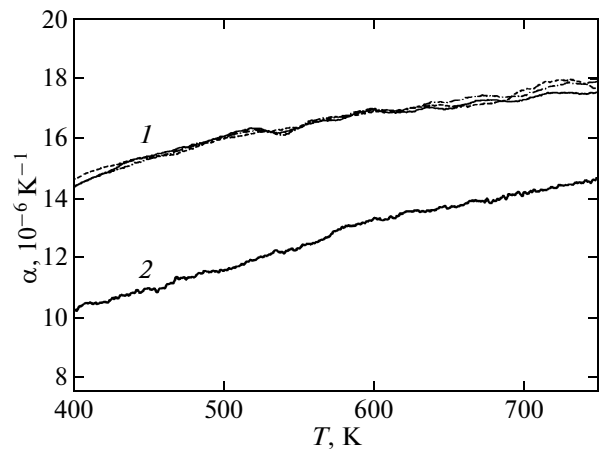


**Fig. 2.** Temperature dependences of the thermal expansion coefficients of the  $\text{SrAlF}_5$  crystal along (1) the  $a$  direction (three successive series of measurements are shown) and (2) the  $c$  direction.

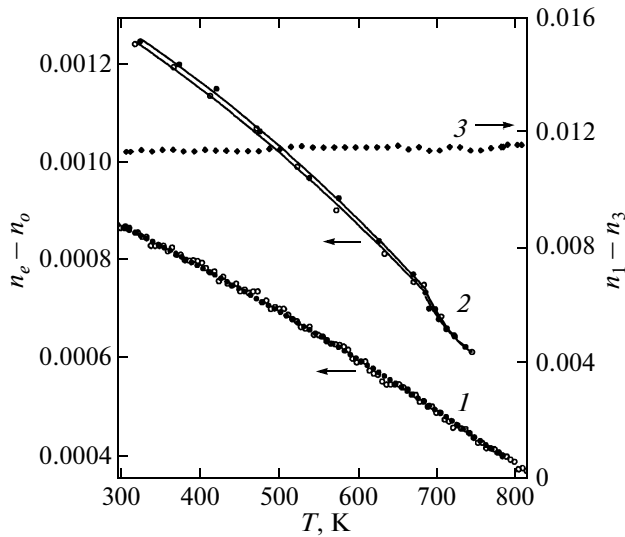


**Fig. 3.** Temperature dependences of the birefringence: (1) main birefringence of SAF in samples nos. 1 and 2 (closed circles, Senarmont compensators) and in sample no. 5 (open circles, Berek compensators), (2) birefringence of SAF according to the experimental data obtained in [11] during heating (closed circles) and cooling (open circles), and (3) birefringence of the AlOF crystal.

the value of the main birefringence is the same in all the five samples studied and is  $(n_e - n_o) = 0.00088$ . The behavior of the birefringence with temperature was studied with the use of the Senarmont compensator on platelets nos. 1 and 2. The results of the measurements turned out identical and reproducible from one heating-cooling cycle to another (Fig. 3, curve 1). All experimental points fit onto a single smooth relation  $(n_e - n_o)(T)$  described by a second-order polynomial. The data points obtained on sample no. 5 with the use of the Berek compensator fit onto the same curve. Thus, the absolute value of the main birefringence and its temperature dependence measured on samples grown in different conditions and by different techniques coincide. Figure 4 plots the temperature dependence  $\Delta(n_e - n_o)/\Delta T$  measured on the matrix part of sample no. 1 (with inclusions) by the high-precision Senarmont method. We readily see that within the 300–800-K region the temperature coefficient of birefringence has no anomalies and follows a linear course.

We used sample no. 2 in an attempt at determining the electromechanical coefficient  $d_{33}$  by the static method. The magnitude of the effect turned out to be two orders of magnitude smaller than that in quartz and in  $\text{SrAlF}_5$  [10], which suggests that the  $d_{33}$  coefficient in our samples is zero. SHG has not also been observed either with the powder sample or with the single crystal. Besides, we have undertaken an attempt at obtaining a dielectric hysteresis loop on the (001) cut of a sample from crystallization no. 2. The result likewise was negative.

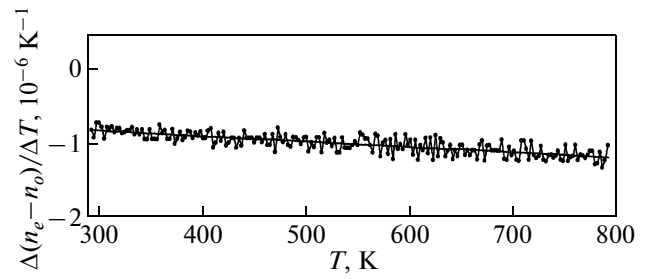


**Fig. 4.** Dependence of  $\Delta(n_e - n_o)/\Delta T$  on the temperature for sample no. 1.

### 3. DISCUSSION

Figure 3 (curve 2) plots for comparison the results of earlier studies of SAF birefringence [11]. Our results (curve 1) are seen to be in striking contrast with literature (curve 2). First, there is a substantial difference between the absolute values of room-temperature birefringence in the compounds investigated. Second, the slopes of the curves are different. Third, the bend in the  $\Delta n(T)$  curve observed [11] in the region of 700 K is attributed to the ferroelectric-paraelectric phase transition. Turning to the first difference from the data of [11], we can note that the absolute room-temperature birefringence measured by us on bulk samples by the Senarmont and Berek methods ( $\Delta n = 0.000879$ ,  $\lambda = 6328 \text{ \AA}$ ) coincides with the data [8] ( $\Delta n = 0.000882$ ,  $\lambda = 6438 \text{ \AA}$ ) derived from measurements of refraction index dispersion by the prism technique. It thus follows that the birefringence of this crystal is very small. With such a weak optical anisotropy and small thickness of the samples used in [11] ( $d \approx 0.1 \text{ mm}$ ), the error of measurements, even with the best modern Berek compensator, can turn out not less than 10%. We believe that the measurements on the thin sample reported in [11] also account for the error in the slope of the  $\Delta n(T)$  curve.

Our experiments have led to quite unexpected findings, namely, in contrast to [11], we did not reveal any anomalies in birefringence in the matrix part of crystal no. 1 and in samples nos. 2 and 5 in the 300–800-K temperature region. Neither were there also found any anomalies in the thermal expansion coefficients within the temperature region covered. Both these experiments are interrelated, because the temperature dependence of refractive indices is determined by the sum of the thermo-optic effect and the elasto-optic contribution originating from thermal expansion of the crystal. The results of the studies suggest also that the material under investigation, most probably, does not undergo any structural phase transitions in the 300–800-K region.

To settle these inconsistencies, we carried out X-ray diffraction studies aimed at determining the chemical composition of the crystal and its structural characteristics. We chose for experiment a transparent, clean piece of matrix material with a linear dimension of



## REFERENCES

1. M. Weil, E. Zobetz, F. Werner, and F. Kubel, *Solid State Sci.* **3**, 441 (2001).
2. J. Ravez and P. Hagenmuller, *Bull. Soc. Chim. Fr.* **7**, 2545 (1967).
3. M. Weil, *Z. Anorg. Allg. Chem.* **627**, 2669 (2001).
4. K. Shimamura, E. G. Villora, K. Muranatsu, and N. Ichinose, *J. Cryst. Growth* **275**, 128 (2005).
5. H. P. Jenssen and S. T. Lai, *J. Opt. Soc. Am. B* **3**, 115 (1986).
6. M. A. Dubinskii, K. L. Schpler, V. V. Semashko, R. Y. Abdulsabirov, S. L. Korableva, and A. K. Naumov, *J. Mod. Opt.* **45** (2), 221 (1998).
7. E. van der Kolk, P. Dorenbos, C. W. E. van Eijk, A. P. Vink, M. Weil, and J. P. Chaminade, *J. Appl. Phys.* **95**, (12) 7867 (2004).
8. E. G. Villora, K. Shimamura, K. Muramatsu, S. Takekawa, K. Kitamura, and N. Ichinose, *J. Cryst. Growth* **280**, 145 (2005).
9. R. von der Mühl, S. Andersson, and J. Gali, *Acta Crystallogr., Sect. B: Struct. Crystallogr. Cryst. Chem.* **27**, 2345 (1971).
10. S. C. Abrahams, J. Ravez, A. Simon, and J. P. Chaminade, *J. Appl. Phys.* **52** (7), 4740 (1981).
11. S. Canouet, J. Ravez, and P. Hagenmuller, *J. Fluorine Chem.* **27**, 241 (1985).
12. F. Kubel, *Z. Anorg. Allg. Chem.* **624**, 1481 (1998).
13. E. N. Silva, A. P. Ayala, J. M. Filho, R. L. Moreira, and J.-Y. Geskand, *J. Phys.: Condens. Matter* **16**, 7511 (2004).
14. E. N. Silva, A. P. Ayala, R. L. Mareira, and J.-Y. Geskand, *J. Phys.: Condens. Matter* **18**, 2511 (2006).
15. J. P. Meehan and E. J. Wilson, *J. Cryst. Growth* **15**, 141 (1972).
16. A. D. Vasiliev, S. V. Melnikova, and L. I. Isaenko, *Acta Crystallogr., Sect. C: Cryst. Struct. Commun.* **65**, i20 (2009).

*Translated by G. Skrebtsov*